Iranian Journal of Physics Research, Vol. 21, No. 3, 2021

Theoretical calculations of the alpha decay half-lives of $^{166-190}$Pt

W A Yahya
Department of Physics and Materials Science, Kwara State University, Malete, Nigeria

E-mail: wasiu.yahya@gmail.com

(Received 06 April 2021 ; in final form 15 July 2021)

Abstract

Calculations of the α-decay half-lives of $^{166-190}$Pt isotopes have been carried out using the modified Gamow-like model (MGLM) and deformed Woods-Saxon potential model. In order to see the effect of using deformed nuclear potential on the α-decay half-lives of the Platinum isotopes, the spherical Woods-Saxon potential has also been employed in the computation. When compared with experimental data, all the models give very good descriptions of the experimental half-lives. The comparison also suggests that the calculated half-lives considering deformation give better agreement with the experimental data than the results using spherical configuration. New parameter values were obtained for the MGLM model (termed MGLM2). The MGLM2 model gives better descriptions of the half-lives than the MGLM1 model.

Keywords: spontaneous nucleation method, KTP crystals, energy gap, transmission spectrum, flux method

1. Introduction

One of the most important decay modes of radioactive nuclei is alpha decay [1, 2]. This decay mode provides nuclear structure information, identification and stability of both heavy and superheavy nuclei [3–5]. Various theoretical models have been employed to investigate the α-decay half-lives for heavy and superheavy nuclei. Some of the models are the cluster formation model [6–11], the generalised liquid drop model [12–14], the modified generalized liquid drop model [4, 15, 16], the fission-like model [17], the effective liquid drop model [18], and the preformed cluster model [19, 20]. The models make use of different interactions ranging from the phenomenological potential such as the proximity potentials, Woods-Saxon, etc, to microscopic interactions like the deformed density dependent potential. Some empirical formulas, such as the universal decay law developed by Qi et al. [21, 22], the scaling law of Horoi [23], scaling law of Brown, the Royer formula [24–26], the Akrawy formula [27], the Ren formula, [28, 29], Viola-Seaborg formula [30], have also been introduced to compute the α-decay half-lives of many isotopes.

Following the work of Zdeb et al. [2], Cheng et al. [3] presented the modified Gamow-like model, by using an improved interaction. The model takes the centrifugal interaction into consideration. This potential model is used to calculate the α-decay half-lives of the Pt isotopes in this study. The three adjustable parameters in the model viz. the radius constant r_0, the hindrance factor h and the screening parameter a of the modified interaction are computed for the $^{166-190}$Pt isotopes. The parameters are fully described in the following Section.

The modified Gamow-like model has been employed to compute the alpha-decay half-lives of $^{171-189}$Hg in Ref. [31]. We have also used the phenomenological Woods-Saxon potential including the deformed Woods-Saxon potential. The results of the calculations are compared with experimental data.

The alpha decay study of the Pt isotopes has been carried out both experimentally and theoretically [32-34]. Pt is known to be a transitional nucleus, and it is found to be deformed in its ground state [32]. Platinum isotopes have been selected for the study because they have non-zero quadrupole and hexadecapole deformation parameters. This will aid to study the effect of using deformed models on the alpha decay half-lives. In previous theoretical alpha decay studies of the Pt isotopes [32-34], spherical nuclear potentials were

employed. This work studies the effect of using deformed nuclear potential on the alpha-decay half-lives of $^{166-190}$Pt isotopes. Therefore both spherical and deformed nuclear potentials will be employed in this work to study the importance of using deformed nuclear potentials.

The paper is organised as follows. In Section 2, the models employed for the calculation of the α-decay half-lives of the Pt isotopes are presented; the modified Gamow-like model and the deformed Woods-Saxon model. The results of the calculations are presented and discussed in Section 3 while the conclusion is given in Section 4.

2. Theory

2.1. Modified Gamow-like model (MGLM)

The interaction potential between the alpha particle and daughter nucleus, in the modified Gamow-like model, is given by [3, 31]

$$V(r) = \begin{cases} -V_0, & 0 \le r \le R_w \\ V_H(r) + V_\ell(r), & r \ge R_w. \end{cases} \quad (1)$$

Here, V_0 denotes the depth of the square well, and the Hulthen type of screened electrostatic Coulomb potential is given by

$$V_H = \frac{aZ_1Z_2e^2}{e^{ar}-1}. \quad (2)$$

The centrifugal potential is

$$V_\ell(r) = \frac{\left(\ell+\frac{1}{2}\right)^2\hbar^2}{2\mu r^2}, \quad (3)$$

Z_1 and Z_2 are the proton numbers of the α particle and daughter nucleus, respectively, the orbital angular momentum taken away by the a particle is denoted by ℓ, and a is the screening parameter. The radius of the spherical square well is obtained by summing the radii of both the a particle (A_1) and the daughter nucleus (A_2):

$$R_w = r_0\left(A_1^{1/3} + A_2^{1/3}\right), \quad (4)$$

where r_0 is an adjustable parameter.

The half-life is then computed using [2, 3]:

$$T_{1/2} = \frac{\ln 2}{vP}10^h, \quad (5)$$

where h is called the hindrance factor. It is due to the effect of an odd-proton and/or an odd-neutron. For even-even nuclei, $h = 0$, and for odd-odd nuclei, $h_{np} = 2h$. The values of r_0, a, and h were determined, in Ref. [3], to be:

$$r_0 = 1.14\,\text{fm},\ a = 7.8\times10^{-4}\,\text{fm}^{-1},\ h = 0.3455. \quad (6)$$

The frequency of assault on the potential barrier (v) is computed by using [3]

$$v = \frac{(G+3/2)\hbar}{1.2\pi\mu R_0^2}, \quad (7)$$

R_0 where the parent nucleus radius is obtained using [3]

$$R_0 = 1.28A^{1/3} - 0.76 + 0.8A^{-1/3}. \quad (8)$$

and the main quantum number G is calculated using [3]

$$G = \begin{cases} 22 & N > 126 \\ 20 & 82 < N \le 126 \\ 18 & N \le 82 \end{cases} \quad (9)$$

The penetration probability (P) is calculated using:

$$P = \exp\left[-\frac{2}{\hbar}\int_{R_w}^{b}\sqrt{2\mu\left(V(r)-E_k\right)}\,dr\right] \quad (10)$$

where, $\mu = mA_1A_2/(A_1+A_2)$ MeV is the reduced mass of the daughter nucleus and the α particle, $m = 931.494$ MeV is the nucleon mass, $E_k = Q_\alpha(A-4)/A$ is the kinetic energy of the emitted α particle, and Q_α is the energy released in the alpha decay process. The classical turning point b is obtained through the condition $V(b) = E_k$.

2. 2. Deformed Woods-Saxon potential (DWS)

In this model, the effective interaction potential between the alpha particle and the deformed daughter nucleus is given by the sum of the deformed nuclear potential $\left(V_N(r,\theta)\right)$, the deformed Coulomb potential $\left(V_C(r,\theta)\right)$ and the centrifugal term $\left(V_\ell(r)\right)$ [35]:

$$V(r,\theta) = V_N(r,\theta) + V_C(r,\theta) + V_\ell(r). \quad (11)$$

Here, ℓ is the angular momentum carried by the α particle and θ is its orientation angle with respect to the symmetry axis of the daughter nucleus. The deformed Woods-Saxon potential is defined as

$$V_N(r,\theta) = \frac{V_0}{1+\exp\left[\frac{r-R(\theta)}{a}\right]}, \quad (12)$$

where the potential depth is obtained via [35, 36]

$$V_0 = -44.16\left[1-0.40I_2\right]\frac{A_2^{2/3}A_1^{2/3}}{A_2^{2/3}+A_1^{2/3}}. \quad (13)$$

Here, the diffuseness parameter is obtained using the formula [38]:

$$a = 0.5 + 0.33I_2, \quad (14)$$

where $I_2 = (N_2 - Z_2)/A_2$ is the relative neutron excess of the daughter nucleus. The daughter nucleus effective radius $R(\theta)$ is given by:

$$R(\theta) = 1.17 + R_2\left[1+\beta_2\mathcal{Y}_{20}(\theta)+\beta_4\mathcal{Y}_{40}(\theta)\right], \quad (15)$$

where β_2 and β_4 are the quadrupole and hexadecapole deformation parameters of the daughter nucleus, respectively, $\mathcal{Y}_{\ell m}(\theta)$ is the spherical harmonics, and

$$R_2 = \left(1+0.39I_2\right)A_2^{1/3} \quad (16)$$

is the radius of the daughter nucleus. It is known that the inclusion of the quadrupole deformation parameter causes a decrease in the half-life calculated value by $2-7$ orders of magnitude [39, 40]. Due to reflection symmetry, the calculations have been carried out by

considering the relative orientations $\theta = 0^\circ - 180^\circ$ with respect to the symmetry axis of the deformed nucleus. The deformed Coulomb potential and the centrifugal term have been computed using

$$V_C(r,\theta) = \frac{Z_1 Z_2 e^2}{r}\left[\begin{matrix}1+\frac{3R^2(\theta)}{5r^2}\beta_2 \mathcal{Y}_{20}(\theta)\\ +\frac{3R^4(\theta)}{9r^2}\beta_4 \mathcal{Y}_{40}(\theta)\end{matrix}\right], \quad (17)$$

$$V_\ell(r) = \frac{\hbar^2 \ell(\ell+1)}{2\mu r^2}, \quad (18)$$

respectively. Here μ is the reduced mass of the α particle and the deformed daughter nucleus. The WKB barrier penetration probability P is calculated via [35, 41]

$$P = \frac{1}{2}\int_0^\pi T_\ell \sin\theta \,||\, d\theta, \quad (19)$$

where the transmission coefficient is evaluated using

$$T_\ell(\theta) = \frac{1}{1+\exp\left[\frac{2}{\hbar}\int_{r_1(\theta)}^{r_2(\theta)}\sqrt{2\mu\left[V(r,\theta)-Q\right]}\,|dr\right]}, \quad (20)$$

where the turning points $r_1(\theta)$ and $r_2(\theta)$ are determined by using the condition $V(r,\theta) = Q$. The α-decay half-life is then computed using

$$T_{1/2} = \frac{\ln 2}{\nu P}, \quad (21)$$

where the assault frequency ν is calculated via [35]

$$\nu = \frac{2E_\nu}{\hbar} = \frac{Q\left[0.056 + 0.039\exp\left(\frac{4-A_2}{2.5}\right)\right]}{\hbar}. \quad (22)$$

For the spherical Woods-Saxon case (SWS), the effective potential between the alpha and daughter nuclei is given by

$$V(r) = V_N(r) + V_C(r) + V_\ell(r), \quad (23)$$

where the nuclear potential

$$V_N(r) = \frac{V_0}{1+\exp\left[\frac{r-R_s}{a}\right]}, \quad (24)$$

and the Coulomb potential is defined as

$$V_C(r) = \frac{Z_1 Z_2 e^2}{r}. \quad (25)$$

In equation (24), R_s is defined as

$$R_s = 1.17 + \left(1 + 0.39 I_2\right) A_2^{1/3}. \quad (26)$$

V_0, a, $T_{1/2}$, and ν are as given in equations (13), (14), (21), and (22), respectively. However, the penetration probability is given here as:

$$P = \exp\left[-\frac{2}{\hbar}\int_{r_1}^{r_2}\sqrt{2\mu\left(V(r)-Q\right)}\,]dr\right]. \quad (27)$$

3. Results and Discussions

In this Section, we present the results of the α-decay half-lives calculations for the $^{166-190}$Pt isotopes. The codes used to do all calculations were written in PYTHON programming language. The calculations have been carried out using the modified Gamow-like model (MGLM) and the deformed Woods-Saxon potential. The calculations using the spherical Woods-Saxon nuclear potential has been included in order to see the effect of using deformed nuclear and Coulomb potentials on the alpha-decay half-lives of the platinum isotopes. In the case of the modified Gamow-like model, we have used the parameters of Ref. [3]; this is denoted as MGLM1. We have also determined the variable parameters in the MGLM (denoted as MGLM2) through a least square fit to the experimental data. The calculated parameters for the MGLM2 are

$$r_0 = 1.2035\,]\text{fm}, \; h = 0.1551, \; a = -7.4459\times10^{-4}\,]\text{fm}^{-1} \quad (28)$$

The experimental data used in the calculations were taken from the NUBASE 2016 database [42- 44], and the following formula was used to calculate the reaction Q_α value [45]:

$$Q_\alpha = \Delta M_P - \Delta M_D - \Delta M_\alpha + k\left(Z_P^\varepsilon - Z_D^\varepsilon\right), \quad (29)$$

Where ΔM_P, ΔM_α, and ΔM_D denote the mass excesses of the parent nucleus, the alpha particle, and the daughter nucleus, respectively. The term $k\left(Z_P^\varepsilon - Z_D^\varepsilon\right)$ denotes the screening effect of atomic electrons [46]; $k = 8.7\,]eV$, $\varepsilon = 2.517$ for $Z \geq 60$, and $k = 13.6\,]eV$, $\varepsilon = 2.408$ for $Z < 60$ [47]. The angular momentum ℓ are determined from the selection rule given by [29, 48, 49]:

$$\ell = \begin{cases}\Delta_j & \text{for even } \Delta_j \text{ and } \pi_d = \pi_p\\ \Delta_j + 1 & \text{for odd } \Delta_j \text{ and } \pi_d = \pi_p\\ \Delta_j & \text{for odd } \Delta_j \text{ and } \pi_d \neq \pi_p\\ \Delta_j + 1 & \text{for even } \Delta_j \text{ and } \pi_d \neq \pi_p\end{cases}, \quad (30)$$

where $\Delta_j = \left|j_p - j_d\right|$, and j_d, π_d, j_p, π_p are the spin and parity values of the daughter and parent nuclei, respectively.

The calculated alpha-decay half-lives for the $^{166-190}$Pt isotopes are shown in Table 1. The first five columns show the mass number (A), the angular momentum carried by the alpha particle (ℓ), the experimental Q_α values, the quadrupole β_2, and the hexadecapole (β_4) deformation parameters, respectively. The experimental α-decay half-lives (Expt.) $\left(\log\left[T_{1/2}(s)\right]\right)$ are shown in the sixth column. The seventh to tenth columns of the Table show the calculated α-decay half-lives using the MGLM1, MGLM2, DWS, and SWS, respectively. A physical inspection shows that all the models give very good descriptions of the half-lives.

However, in order to quantitatively compare the agreement between the experimental and theoretically calculated half-lives, the root mean square standard

Table 1. Calculated α-decay half-lives, $\log\left[\mathrm{T}_{1/2}(\mathrm{s})\right]$, of Pt isotopes $(Z=78)$ using MGLM1, MGLM2, DWS, and SWS. $\log\left[\mathrm{T}_{1/2}(\mathrm{s})\right]$.

A	ℓ	Q	β_2	β_4	Expt	MGLM1	MGLM2	DWS	SWS
166	0	7.3177	0.1070	-0.0080	-3.5232	-3.5048	-3.7173	-3.1904	-3.1432
167	0	7.1871	0.1180	-0.0070	-3.1546	-2.7783	-3.1686	-2.8299	-2.7716
168	0	7.0216	0.1290	0.0060	-2.6968	-2.6187	-2.8016	-2.3458	-2.2703
170	0	6.7393	0.1510	-0.0040	-1.8516	-1.7165	-1.8677	-1.4816	-1.3802
171	0	6.6392	0.1620	-0.0150	-1.3486	-1.0425	-1.3720	-1.1770	-1.0628
172	0	6.4952	0.1730	-0.0130	-0.8935	-0.8909	-1.0114	-0.7019	-0.5695
173	0	6.3867	0.1730	-0.0130	-0.3517	-0.1640	-0.4602	-0.3309	-0.1967
174	0	6.2150	0.1840	-0.0120	0.0685	0.1286	0.0479	0.2894	0.4439
175	2	6.1954	0.1840	-0.0120	0.5960	0.7802	0.5038	0.5963	0.7597
176	0	5.9169	0.1950	-0.0100	1.2226	1.3011	1.2688	1.4372	1.6172
177	0	5.6748	0.2060	-0.0090	2.3284	2.6844	2.5068	2.4685	2.6743
178	0	5.6048	0.2170	-0.0070	2.4504	2.6367	2.6630	2.7299	2.9608
179	2	5.4442	0.2170	-0.0070	3.9463	3.9710	3.8334	3.7408	3.9874
180	0	5.2690	0.2180	-0.0190	4.2395	4.2158	4.3163	4.3267	4.5589
181	0	5.1819	0.2180	-0.0190	4.8474	4.9871	4.9183	4.7447	4.9794
182	0	4.9828	0.2190	-0.0310	5.5405	5.6864	5.8609	5.8091	6.0447
183	0	4.8540	0.2190	-0.0310	6.6097	6.7358	6.7571	6.5164	6.7555
184	0	4.6305	0.2190	-0.0430	7.7869	7.6990	7.9822	7.8543	8.0964
186	0	4.3516	0.2200	-0.0560	9.7270	9.4605	9.8465	9.6356	9.8884
188	0	4.0386	0.2200	-0.0680	12.5285	11.6640	12.1882	11.8775	12.1434
190	0	3.3004	0.2090	-0.0830	19.2315	18.1334	19.1280	18.5877	18.8622

deviation σ has been computed using:

$$\sigma=\sqrt{\frac{1}{N}\sum_{i=1}^{N}\left[\left(\log_{10}T_{1/2,i}^{\mathrm{Theory}}-\log_{10}T_{1/2,i}^{\mathrm{Expt}}\right)^2\right]}, \qquad (31)$$

where $T_{1/2,i}^{\mathrm{Expt}}$ are the experimental half-lives, and $T_{1/2,i}^{\mathrm{Theory}}$ are the half-lives calculated using the theoretical models. The results of the standard deviation (σ) calculations using the different models are shown in Table 2 The standard deviation values for the MGLM1, MGLM2, DWS, and SWS, are 0.3512, 0.1528, 0.2868, and 0.3389, respectively. From these values, one observes that the DWS model gives the lowest standard deviation when compared to the SWS and MGLM1 models. This shows the importance of using a deformed nuclear potential over the spherical one for these Platinum isotopes. The MGLM2 model, seen to give the lowest deviation has been obtained through a fit of the variable parameters to experimental data. This simple model has been shown to give excellent descriptions of α-decay half-lives [3, 31].

Figure 1 shows the plots of the computed α-decay half-lives, $\log\left[T_{1/2}(s)\right]$, using the four theoretical models against the neutron number (N). The experimental values are shown in black squares. The half-life can be seen to increase with increase in neutron number for the series of isotopes considered in the study. One observes from the figure that all the models give very good descriptions of the alpha decay half-lives, since only a slight difference between the calculated results and experimental can be seen. The difference between experimental and theoretical α-decay half-lives have been obtained using the following equation:

$$\Delta T_{1/2}=\log_{10}\left[T_{1/2}^{\mathrm{theor}}\right]-\log_{10}\left[T_{1/2}^{\mathrm{expt}}\right]. \qquad (32)$$

$\Delta T_{1/2}$ has been plotted against neutron number in Figure 2 for the four models used in the study. It can be observed that, barring few exceptions, most of the points are near zero and within ± 0.5. For instance, the MGLM2 model gives $\Delta T_{1/2}$ values less than ± 0.5. Moreover, it can be observed that the DWS model gives lower $\Delta T_{1/2}$ values than the SWS model. This shows the

Table 2. Calculated root means square standard deviation (σ) using the different models.

Model	σ
MGLM1	0.3512
MGLM2	0.1528
DWS	0.2868
SWS	0.3389

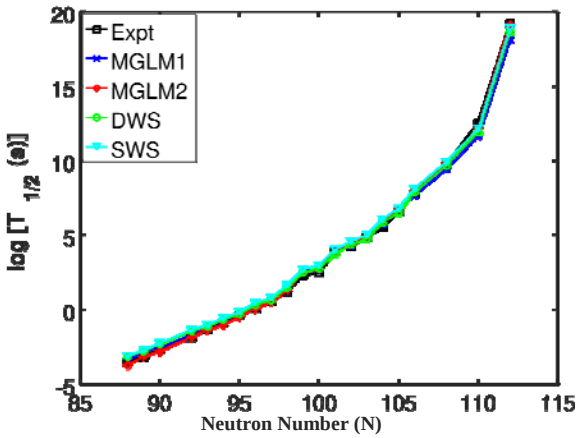

Figure 1. Plots of the calculated α-decay half-lives of Pt isotopes between the various models and experiment.

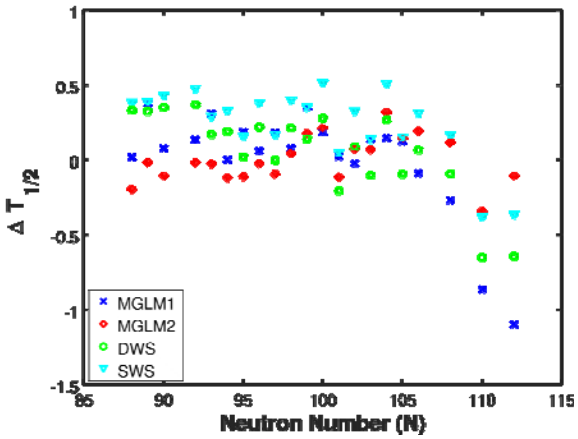

Figure 2. Plots of the ΔT against Neutron number (N) for the Pt isotopes using the different models.

advantage of using deformed model for the Pt isotopes. Also, comparing the $\Delta T_{1/2}$ values between the MGLM1 and MGLM2, it can be seen that the MGLM2 gives lower $\Delta T_{1/2}$ than the MGLM1 model.

Conclusion

The theoretical study of the α-decay half-lives of $^{166-190}$Pt isotopes have been carried out using the modified Gamow-like model (MGLM1) and deformed Woods-Saxon potential model (DWS). Calculations using spherical Woods-Saxon potential (SWS) were included to see the effect of using deformed nuclear potential on the α-decay half-lives of the Platinum isotopes. All the models give very good descriptions of the α-decay half-lives when compared with experimental data. The computed standard deviation indicates that the calculated half-lives using deformed nuclear and Coulomb potentials give better agreement with the experimental data than the results using spherical nuclear and Coulomb potentials. New parameter values were obtained for the MGLM model (termed MGLM2). The MGLM2 model gives better descriptions of the half-lives than the MGLM1 model. In general, all the models give α-decay half-lives which are in good agreement with the available experimental data, with maximum standard deviation value less than 0.4. The difference between theoretically calculated and experimental α-decay half-lives is also found to be less than ±0.5 for most of the isotopes. The results showed the importance of using deformed nuclear potentials over spherical ones for the Pt isotopes, because the deformed configuration gave lower deviation from experimental data than the spherical configuration.

Acknowledgement

The author appreciates the reviewers for valuable comments.

References

1. E Shin, Y Lim, C H Hyun, and Y Oh, *Physical Review* C **94** (2016) 024320.
2. A Zdeb, M Warda, and K Pomorski, *Physical Review* C **87** (2013) 024308.
3. J-H Cheng *et al*., *Nuclear Physics* A **987** (2019) 350.
4. K P Santhosh, D T Akrawy, H Hassanabadi, A H Ahmed, and T A Jose, *Physical Review* C **101** (2020) 064610.
5. N A M Alsaif, S Radiman, and S M S Ahmed, *International Journal of Modern Physics* E **26** (2017) 1750008.
6. J-G Deng, J-C Zhao, P-C Chu, and X-H Li, *Physical Review* C **97** (2018) 044322.
7. S M S Ahmed, R Yahaya, and S Radiman, *Romanian Reports in Physics* **65** (2013) 1281.
8. D Deng, Z Ren, D Ni, and Y Qian, *Journal of Physics G: Nuclear and Particle Physics* **42** (2015) 075106.
9. S M S Ahmed, R Yahaya, S Radiman, and M S Yasir, *Journal of Physics G: Nuclear and Particle Physics* **40** (2013) 065105.
10. D Deng and Z Ren, *Physical Review* C **93** (2016) 044326.
11. S M S Ahmed, *Nuclear Physics* A **962** (2017) 103.

12. G Royer and R Moustabchir, *Nuclear Physics* A **683** (2001) 182.
13. B Xiaojun, H Zhang, H Zhang, G Royer, and J Li, *Nuclear Physics* A **921** (2014) 85.
14. G Royer and H F Zhang, *Physical Review* C **77** (2008) 037602.
15. K P Santhosh, C Nithya, H Hassanabadi, and D T Akrawy, *Physical Review* C **98** (2018) 024625.
16. K P Santhosh and T A Jose, *Nuclear Physics* A **992** (2019) 121626.
17. Y J Wang, H F Zhang, W Zuo, and J Q Li, *Chinese Physics Letter* **27** (2010) 062103.
18. J P Cui, Y L Zhang, S Zhang, and Y Z Wang, *Physical Review* C **97** (2018) 014316.
19. R K Gupta and W Greiner, *International Journal of Modern Physics* E **3** (1994) 335.
20. B B Singh, S K Patra, and R K Gupta, *Physical Review* C **82** (2010) 014607.
21. C Qi *et al*., *Physical Review* C **80** (2009) 044326.
22. C Qi, F R Xu, R J Liotta, and R Wyss, *Physical Review Letters* **103** (2009) 072501.
23. M Horoi, *Journal of Physics G: Nuclear and Particle Physics* **30** (2004) .
24. G Royer, *Journal of Physics G: Nuclear and Particle Physics* **26** (2000) 1149.
25. G Royer, Nuclear Physics A **848** (2010) 279.
26. G Royer, C Schreiber, and H Saulnier, *International Journal of Modern Physics* E **20** (2011) 1030.
27. D T Akrawy and A H Ahmed, *International Journal of Modern Physics* E **27** (2018) 1850068.
28. Z. Ren, C. Xu, and Z. Wang, Physical Review C **70**, 034304 (2004).
29. D T Akrawy, H Hassanabadi, Y Qian, and K P Santhosh, *Nuclear Physics* A **983** (2019) 310.
30. V Viola and G Seaborg, *Journal of Inorganic and Nuclear Chemistry* **28** (1966) 741.
31. W A Yahya, *Journal of the Nigerian Society of Physical Sciences* **2** (2020) 250.
32. N Ashok and A Joseph, *International Journal of Modern Physics* E **27** (2018) 1850098.
33. O A P Tavares and E L Medeiros, *Physica Scripta* **84** (2011) 045202.
34. S S Hosseini, H Hassanabadi, and H Sobhani, *International Journal of Modern Physics* E **26** (2017) 1750069.
35. M Pahlavani and S Rahimi Shamami, *Chinese Journal of Physics* **66** (2020) 733.
36. J Dudek and T Werner, *J. Phys. G: Nucl. Part. Phys*. **4** (1986) 1543.
37. F Saidi, M R Oudih, M Fellah, and N H Allal, *Mod. Phys. Lett*. A **30** (2015) 1550150.
38. N Wang and W Scheid, *Phys. Rev*. C **78** (2008) 014607.
39. S K Arun, R K Gupta, B B Singh, S Kanwar, and M K Sharma, *Phys. Rev*. C **79** (2009) 064616.
40. G Sawhney, M K Sharma, and R K Gupta, *Phys. Rev.* C **83** (2011) 064610.
41. V Y Denisov and A A Khudenko, *Phys. Rev*. C **80** (2009) 034603.
42. G Audi, F G Kondev, M Wang, W Huang, and S Naimi, *Chinese Physics* C **41** (2017) 030001.
43. M Wang *et al*., *Chinese Physics* C **41** (2017) 030003.
44. W J Huang *et al*., *Chinese Physics* C **41** (2017) 030002.
45. K Santhosh, I Sukumaran, and B Priyanka, *Nuclear Physics* A **935** (2015) 28.
46. V Y Denisov and H Ikezoe, *Physical Review* C **72** (2005) 064613.
47. K N Huang, M Aoyagi, M H Chen, B Crasemann, and H Mark, *Atomic Data and Nuclear Data Tables* **18** (1976) 243.
48. C Qi, D Delion, R Liotta, and R Wyss, *Physical Review* C **92** (2015) 014602.
49. V Denisov, O Davidovskaya, and I Sedykh, *Physical Review* C **85** (2012) 011303.